



Optogenetic Stimulation of Lateral Orbitofronto-Striatal Pathway Suppresses Compulsive Behaviors

Eric Burguière *et al.*

Science **340**, 1243 (2013);

DOI: 10.1126/science.1232380

This copy is for your personal, non-commercial use only.

If you wish to distribute this article to others, you can order high-quality copies for your colleagues, clients, or customers by [clicking here](#).

Permission to republish or repurpose articles or portions of articles can be obtained by following the guidelines [here](#).

The following resources related to this article are available online at www.sciencemag.org (this information is current as of February 27, 2014):

Updated information and services, including high-resolution figures, can be found in the online version of this article at:

<http://www.sciencemag.org/content/340/6137/1243.full.html>

Supporting Online Material can be found at:

<http://www.sciencemag.org/content/suppl/2013/06/05/340.6137.1243.DC1.html>

A list of selected additional articles on the Science Web sites **related to this article** can be found at:

<http://www.sciencemag.org/content/340/6137/1243.full.html#related>

This article **cites 30 articles**, 10 of which can be accessed free:

<http://www.sciencemag.org/content/340/6137/1243.full.html#ref-list-1>

This article has been **cited by** 3 articles hosted by HighWire Press; see:

<http://www.sciencemag.org/content/340/6137/1243.full.html#related-urls>

This article appears in the following **subject collections**:

Neuroscience

<http://www.sciencemag.org/cgi/collection/neuroscience>

Optogenetic Stimulation of Lateral Orbitofronto-Striatal Pathway Suppresses Compulsive Behaviors

Eric Burguière,¹ Patrícia Monteiro,¹ Guoping Feng,¹ Ann M. Graybiel^{1*}

Dysfunctions in frontostriatal brain circuits have been implicated in neuropsychiatric disorders, including those characterized by the presence of repetitive behaviors. We developed an optogenetic approach to block repetitive, compulsive behavior in a mouse model in which deletion of the synaptic scaffolding gene, *Sapap3*, results in excessive grooming. With a delay-conditioning task, we identified in the mutants a selective deficit in behavioral response inhibition and found this to be associated with defective down-regulation of striatal projection neuron activity. Focused optogenetic stimulation of the lateral orbitofrontal cortex and its terminals in the striatum restored the behavioral response inhibition, restored the defective down-regulation, and compensated for impaired fast-spiking neuron striatal microcircuits. These findings raise promising potential for the design of targeted therapy for disorders involving excessive repetitive behavior.

Repetitive behaviors are cardinal features of a number of neuropsychiatric conditions (1, 2). Single behaviors and ritualistic sequences of behavior can be repeated compulsively to the point of seriously interfering with daily functioning (3). Attempts to find efficacious

therapies for such conditions have been challenging (4, 5). Neuroimaging studies have identified abnormalities in cortico-basal ganglia circuits, particularly those involving the orbitofrontal cortex, implicated in the expression of repetitive, compulsive, and impulsive behaviors (6, 7). Dis-

abling the lateral part of the orbitofrontal cortex (IOFC) reduces response inhibition and increases impulsive choice, and this deficit in response inhibition is likely related to abnormalities in orbitofrontal interactions with the striatum and associated basal ganglia circuits (7–10). We targeted this orbito-fronto-striatal system to examine its function and to develop an optogenetic, therapeutic approach to treat compulsive behavior. As a model, we focused on the compulsive behavioral responses exhibited by *Sapap3* mutant mice (11, 12), which exhibit spontaneous, repetitive facial overgrooming and anxiety, behaviors that could be considered analogous to pathological repetitive behaviors in obsessive-compulsive disorder–spectrum disorders (13).

We first asked whether, as is thought to be the case in some human conditions, repetitive behavior in the *Sapap3* mutants could be triggered as an excessive reaction to a neutral stimulus that has been associated with a natural behavioral response. We designed a conditioning paradigm in which a neutral stimulus (a water drop applied to the

¹McGovern Institute for Brain Research and Department of Brain and Cognitive Sciences, Massachusetts Institute of Technology, Cambridge, MA 02139, USA.

*Corresponding author. E-mail: graybiel@mit.edu

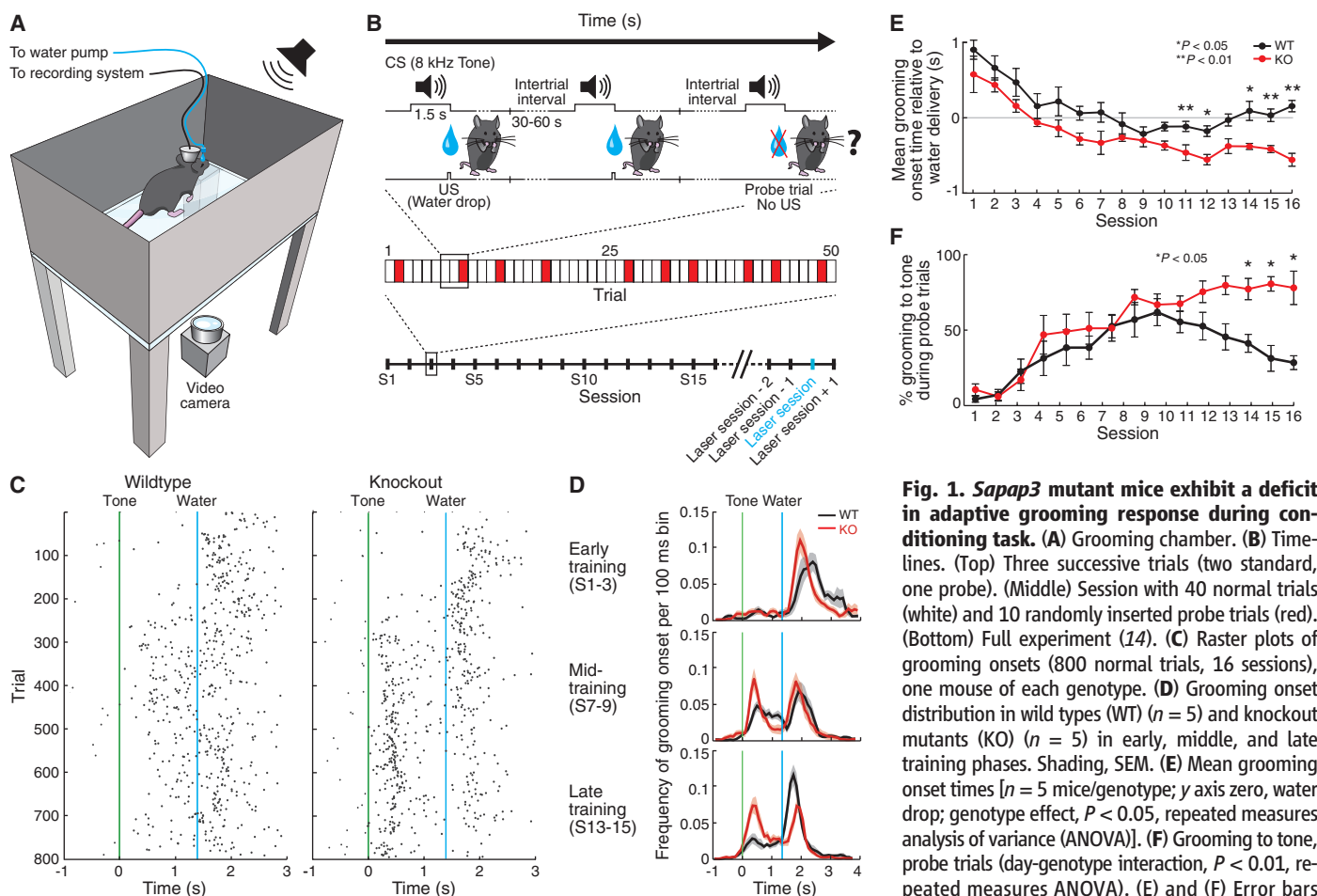


Fig. 1. *Sapap3* mutant mice exhibit a deficit in adaptive grooming response during conditioning task. (A) Grooming chamber. (B) Time-lines. (Top) Three successive trials (two standard, one probe). (Middle) Session with 40 normal trials (white) and 10 randomly inserted probe trials (red). (Bottom) Full experiment (14). (C) Raster plots of grooming onsets (800 normal trials, 16 sessions), one mouse of each genotype. (D) Grooming onset distribution in wild types (WT) ($n = 5$) and knockout mutants (KO) ($n = 5$) in early, middle, and late training phases. Shading, SEM. (E) Mean grooming onset times [$n = 5$ mice/genotype; y axis zero, water drop; genotype effect, $P < 0.05$, repeated measures analysis of variance (ANOVA)]. (F) Grooming to tone, probe trials (day-genotype interaction, $P < 0.01$, repeated measures ANOVA). (E) and (F) Error bars show SEM.

forehead) provoked a grooming response that could be clearly identified, which allowed us to pair a tone with the water drop in a delay-conditioning paradigm (Fig. 1, A and B, and fig. S1) (14).

The behavior of the *Sapap3* mutant mice and their wild-type littermates diverged sharply during the course of conditioning. Early on, both mutants ($n = 7$) and littermate controls ($n = 7$) readily became conditioned, grooming when the conditioning tone was played (Fig. 1, C and D). Later in training, the wild types began to inhibit

this early grooming to the tone onset and to respond immediately after the water-drop release. The *Sapap3* mutants, by contrast, having once acquired the conditioned responses, kept responding to the tones with short-latency grooming, even in probe trials lacking water-drop delivery (Fig. 1, C to F; figs. S2 and S3; and table S1). This emergence of excessive short-latency responses was not accompanied by increased general grooming behavior or by hypersensitivity to the tone (figs. S4 and S5 and supplementary

text). The *Sapap3* mutant mice thus expressed an acquired maladaptive behavior characterized by defective inhibition of their conditioned responses to the originally neutral tone stimuli.

Learning theories of human compulsive behavior suggest that repetitive behaviors can result from malfunction of a learning process that leads to loss of the ability to repress sensorimotor associations (3, 15, 16). To identify the neuronal basis of such a deficit, we recorded spike and local field potential (LFP) activity simultaneously

Fig. 2. Dynamic learning-related changes in IOFC and striatal ensemble activity differ in wild-type and *Sapap3* mutant mice. Average baseline firing rates of IOFC (A) and striatal (E) units. Average activity of IOFC (B to D) and striatal (F to H) units classified as task-responsive (i.e., firing preferentially between tone and water events relative to baseline activity). Mean z-scores normalized for each neuron relative to baseline activity for wild-type (WT) ($n = 7$) and *Sapap3* mutant (KO) ($n = 7$) mice during training. Above, ratios of task-responsive units to total units per genotype. Shading, SEM.

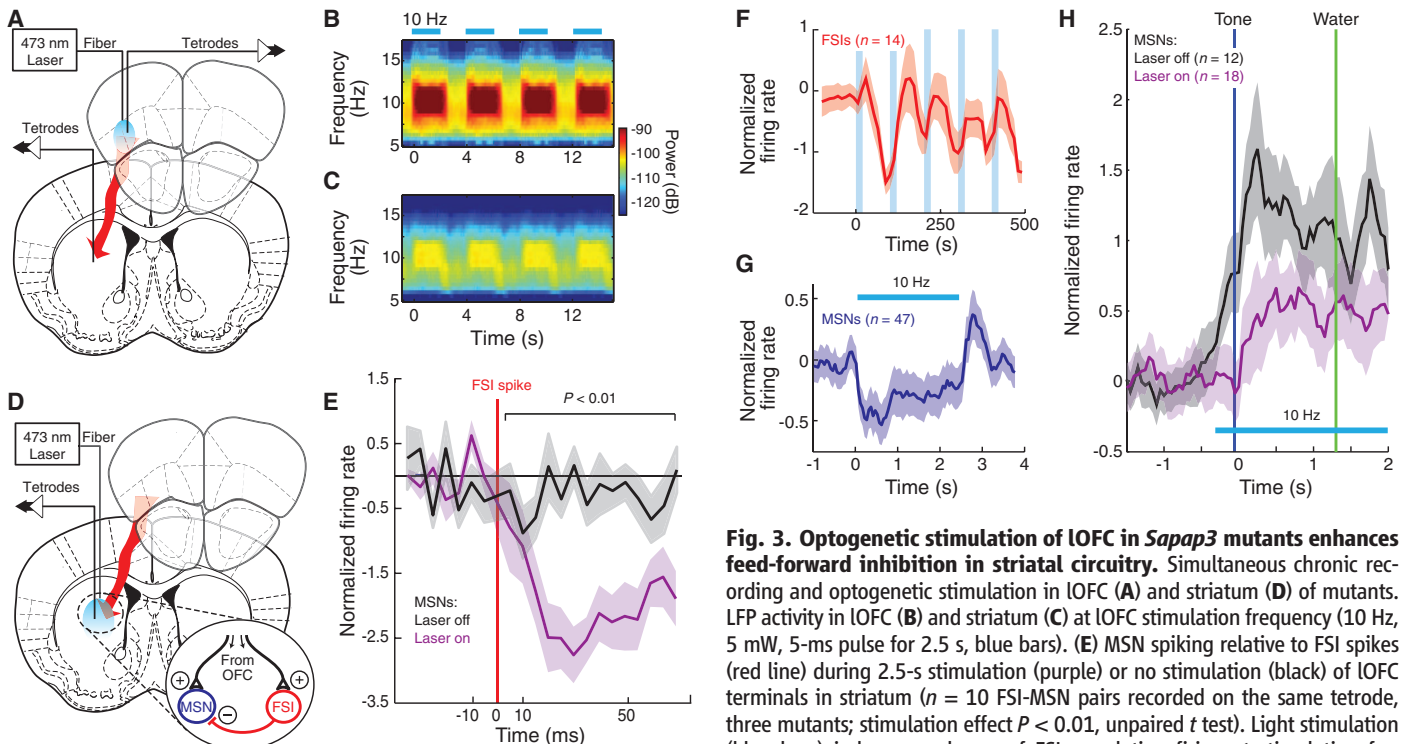
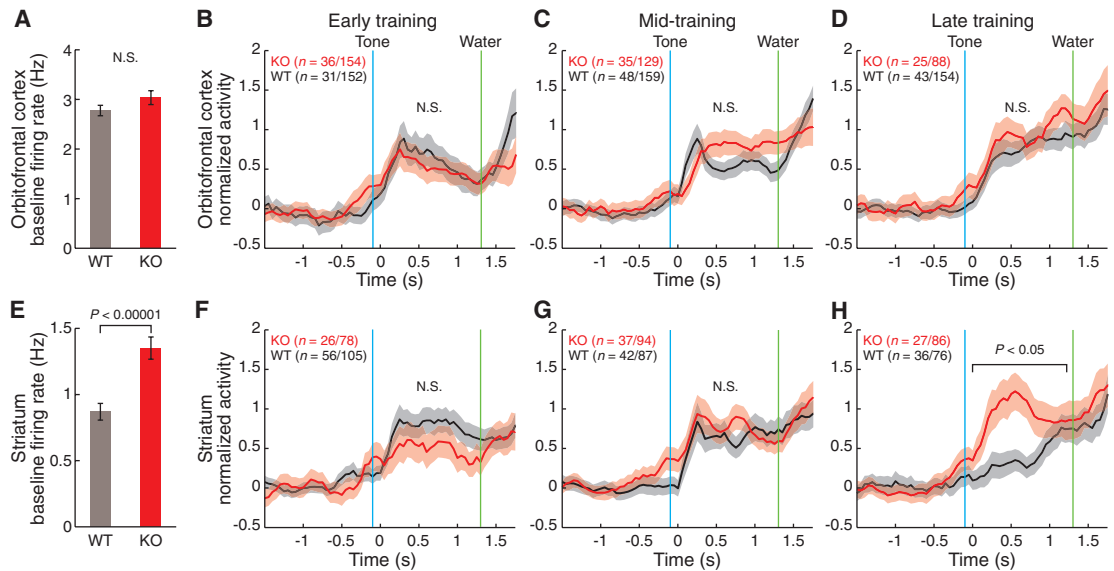


Fig. 3. Optogenetic stimulation of IOFC in *Sapap3* mutants enhances feed-forward inhibition in striatal circuitry. Simultaneous chronic recording and optogenetic stimulation in IOFC (A) and striatum (D) of mutants. LFP activity in IOFC (B) and striatum (C) at IOFC stimulation frequency (10 Hz, 5 mW, 5-ms pulse for 2.5 s, blue bars). (E) MSN spiking relative to FSI spikes (red line) during 2.5-s stimulation (purple) or no stimulation (black) of IOFC terminals in striatum ($n = 10$ FSI-MSN pairs recorded on the same tetrode, three mutants; stimulation effect $P < 0.01$, unpaired t test). Light stimulation (blue bars) induces synchrony of FSI population firing at stimulation frequency (F) ($n = 14$ units, three mutants) and long-lasting inhibition of MSNs during stimulation (G) ($n = 47$ units, three mutants). (H) Same stimulation protocol applied at the end of the training significantly decreased MSNs firing (purple) relative to no-stimulation condition (black). Shading, SEM.

with tetrodes in the IOFC and centromedial striatum as the mice acquired and then performed the task (fig. S6) (14). The baseline raw firing rates of putative pyramidal cells in the IOFC were similar in mutants ($n = 7$) and wild types ($n = 7$) throughout training, but the baseline firing rates of putative medium spiny neurons (MSNs) in the striatum were significantly elevated in the *Sapap3* mutants (Fig. 2, A and E).

During the early stages of training, subpopulations of pyramidal neurons in the IOFC in both genotypes exhibited a significant increase of activity between the tone and water events (Fig. 2B, fig. S7A, and table S2) (14). These IOFC responses remained similar throughout training; activity after the tone became progressively sustained up to the time of water-drop delivery (Fig. 2, B to D). By contrast, striatal task-related MSN activity patterns diverged markedly during training for the mutant and wild-type mice (Fig. 2, F to H, and fig. S7B) (14). Early on, MSNs in both geno-

types exhibited a phasic increase in response to the tone; but the slope of this increase steadily declined in the wild types but did not in the *Sapap3* mutants (Fig. 2H). This tuning of MSN activity in the wild types occurred as their grooming onset times shifted toward the time of water-drop delivery (fig. S8).

The lack of such learning-related MSN tuning in the mutants could have reflected increased excitation or decreased inhibition of activity after the tone (see supplementary text). We considered one powerful source of MSN inhibition, deriving from fast-spiking striatal interneurons (FSIs), which mediate fast feed-forward inhibition of MSNs in response to cortical activation (17) and largely correspond to parvalbumin (PV)-containing interneurons. In cell counts of PV-immunostained sections, we found significantly fewer PV-positive striatal neurons in the mutants than in the wild types ($n = 8$ mice per genotype, chi-square test, $P < 0.05$) (fig. S9) (14).

This result suggested that a defect in intra-striatal inhibition could contribute to the *Sapap3* mutant phenotype but did not identify the source of the abnormality. In the light of clinical evidence (6, 9), we asked whether we could restore the striatal inhibition by optogenetically altering IOFC input to the striatum. We injected the IOFC bilaterally with adeno-associated virus (AAV5) to express a fusion protein of channelrhodopsin-2 and enhanced yellow fluorescent protein (ChR2-EYFP) under the calcium- and calmodulin-dependent protein kinase II (CaMKII) promoter (18) to target cortical pyramidal neurons of *Sapap3* mutant mice (fig. S10). We delivered pulses of blue light (473 nm, 5 mW, 10 Hz pulses) through two independently movable optical fibers and simultaneously recorded neural activity in the IOFC and striatum (Fig. 3, A and D, and fig. S11) (14). We confirmed expression of ChR2 and spike and LFP modulation at the stimulation frequency (Fig. 3, B and C, and figs. S10 and S11). Control experiments with ineffective laser stimulation and with control virus were negative (fig. S12).

We stimulated the ChR2-containing IOFC axon terminals within the striatum while we recorded from ensembles of striatal neurons (Fig. 3D). To assess specifically the direct effect of IOFC stimulation on FSIs and MSNs in the *Sapap3* mutants, we isolated 10 FSI-MSN pairs in which both members of the pair were recorded on the same tetrode (Fig. 3E and figs. S7B and S13) (14). In these recordings, MSN spiking was inhibited after FSI spikes, and this inhibition was greatly increased during optogenetic stimulation of IOFC terminals in the striatum (unpaired t test, $P < 0.01$). This effect could also be seen at the population level (Fig. 3, F and G). These dynamics suggest that activation of the IOFC-striatal pathway in the *Sapap3* mutants compensated for their abnormally high MSN activity at the end of the training by eliciting a powerful feed-forward inhibition of MSNs driven by the cortical activation of FSIs (19).

We applied this IOFC-striatal optogenetic stimulation at the end of training and showed that it could restore MSN tone-response inhibition in the *Sapap3* mutants (Fig. 3H). We then asked whether such stimulation could also ameliorate the behavior of the *Sapap3* mutant mice (Fig. 4, A to D). At the end of the training, we excited either projection neurons in the IOFC or their terminals in the striatum in different experiments, triggering the laser at tone onset and continuing it for 2.5 s at 10 Hz. When the *Sapap3* mutants were under optical stimulation, their early grooming responses to the tones were almost completely abolished, both by IOFC stimulation ($n = 4$) (Fig. 4, A, B, and E) and by striatal stimulation ($n = 3$) (Fig. 4, C to E). Yet the mutants groomed normally as soon as the water drop was delivered. The abnormal stimulus-evoked compulsive behavior in the *Sapap3* mutants thus could have resulted from a deficit of behavioral inhibition that was restored by optogenetically stimulating the IOFC-striatal pathway.

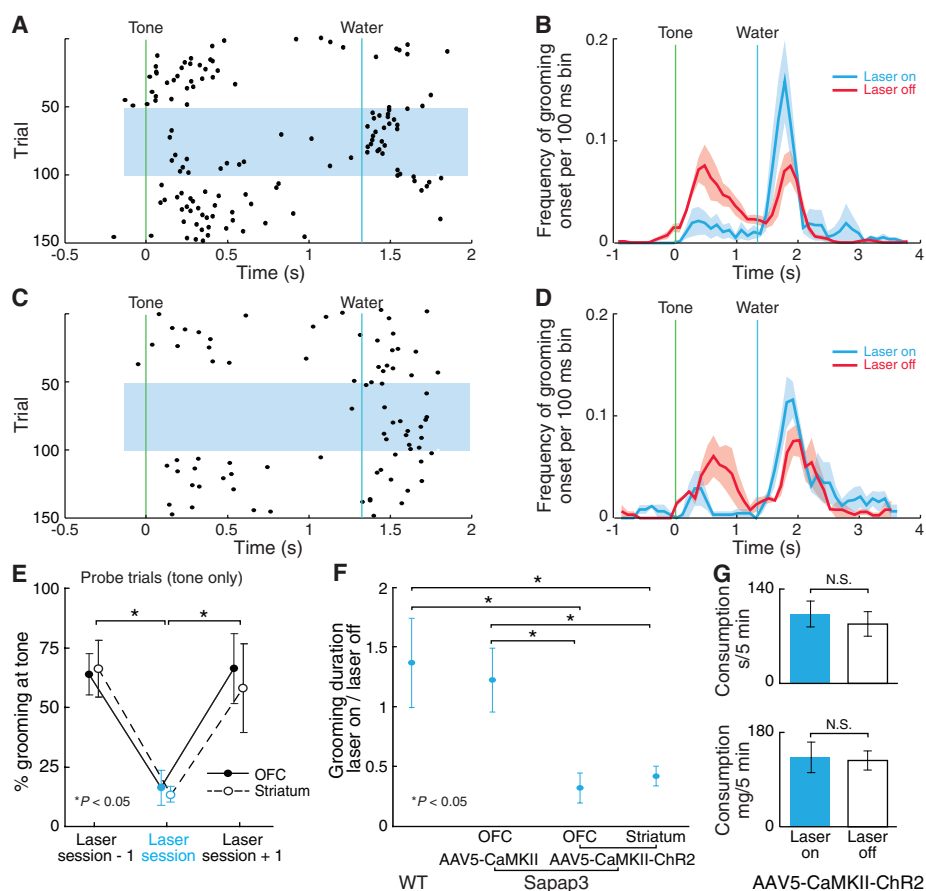


Fig. 4. Optogenetic stimulation of IOFC alleviates compulsive grooming of *Sapap3* mutant mice. Rasters of grooming onsets before, during (blue shading), and after bilateral IOFC (A) or striatal (C) stimulation (10 Hz, 5 mW, 5-ms light pulses) in a *Sapap3* mutant, late in training. Grooming onsets for the *Sapap3* population during session with laser stimulation (blue) in IOFC (B) ($n = 4$) or striatum (D) ($n = 3$) compared with preceding laser-off session (red). Shading, SEM. (E) Suppression of tone-evoked grooming by IOFC or striatal stimulation during probe trials ($P < 0.01$, unpaired t test). (F) Alleviation of compulsive grooming in *Sapap3* mutants ($n = 4$) by IOFC or striatal stimulation (5 Hz, 5 mW, 5-ms light pulses) during 3-min free-movement periods, and control virus ($n = 3$) and wild-type ($n = 3$) comparisons ($P < 0.05$, unpaired t test). (G) Lack of effect of same out-of-task IOFC stimulation in mutants ($n = 4$) on time spent eating (top) or food consumed (bottom) during 5-min free-feeding periods. Error bars in (E to G), SEM.

We next tested whether we could also rescue the spontaneous compulsive phenotype of the *Sapap3* mutants by optogenetically stimulating in IOFC ($n = 6$) or striatum ($n = 4$) during their unconditioned, natural behavior, which is typified by excessive grooming, but for which the triggers impelling the grooming behavior are unknown (Fig. 4F) (14). Stimulation (5 Hz, 5 mW, 5-ms pulse for 3 min) almost fully alleviated their compulsive grooming (Fig. 4F), leaving intact other out-of-task behaviors requiring fine motor coordination and motivation ($n = 5$) (Fig. 4G). Wild types expressing CaMKII-ChR2 ($n = 3$) and *Sapap3* mutants expressing control virus ($n = 3$) showed no difference in grooming with the laser on or off (Fig. 4F).

Our findings demonstrate that selective stimulation of the IOFC-striatal pathway can restore a behavioral inhibition signal in an animal model expressing pathological repetitive behaviors and can prevent overexpression of both conditioned and spontaneous repetitive grooming. Optogenetic stimulation increased inhibition of striatal MSNs in the mutants, and it specifically activated striatal FSIs and affected FSI-MSN striatal microcircuitry. The abnormally elevated MSN baseline firing rates in the *Sapap3* mutant striatum and reduced numbers of PV-immunostained striatal interneurons, likely corresponding to physiologically identified FSIs, suggest that the microcircuit necessary for inhibiting MSN responses through FSI excitation may not have been fully functional (supplementary text) (11, 13).

A pathologic decrease of PV-containing striatal neurons has been observed in Tourette's syndrome, and FSI microcircuits have been implicated in other extrapyramidal disorders (20, 21). Our findings suggest that a key role of the IOFC in

underpinning response inhibition could include specific effects on FSI-MSN microcircuitry by which the IOFC controls striatal neurons (supplementary text).

Our finding that optogenetic control of this IOFC-striatal pathway can alleviate repetitive behaviors in a genetic model of compulsive behavior raises important questions for future work (supplementary text). Are subsystems of striatal MSNs (e.g., D1 and D2 dopamine receptor-expressing neurons or striosome and matrix neurons) differentially affected (22–25)? Can this targeted optogenetic therapy alleviate repetitive behaviors in other models? What microcircuits underlie the normal orbitofronto-striatal pathway neuroplasticity and behavioral adaptation evident in the wild types? Our findings should provide a platform for exploring these differential influences and for developing new potential therapeutic targets to alleviate conditions characterized by abnormally repetitive behavior.

References and Notes

1. J. F. Leckman, *Lancet* **360**, 1577 (2002).
2. R. M. Ridley, *Prog. Neurobiol.* **44**, 221 (1994).
3. M. E. Franklin, E. B. Foa, *Annu. Rev. Clin. Psychol.* **7**, 229 (2011).
4. C. Otte, *Dialogues Clin. Neurosci.* **13**, 413 (2011).
5. W. K. Goodman, R. B. Lydiard, *J. Clin. Psychiatry* **68**, e30 (2007).
6. S. R. Chamberlain *et al.*, *Science* **321**, 421 (2008).
7. M. R. Milad, S. L. Rauch, *Trends Cogn. Sci.* **16**, 43 (2012).
8. D. M. Eagle, C. Baunez, *Neurosci. Biobehav. Rev.* **34**, 50 (2010).
9. A. C. Mar, A. L. Walker, D. E. Theobald, D. M. Eagle, T. W. Robbins, *J. Neurosci.* **31**, 6398 (2011).
10. A. M. Graybiel, S. L. Rauch, *Neuron* **28**, 343 (2000).
11. M. Chen *et al.*, *J. Neurosci.* **31**, 9563 (2011).
12. J. M. Welch *et al.*, *Nature* **448**, 894 (2007).
13. S. Züchner *et al.*, *Mol. Psychiatry* **14**, 6 (2009).
14. Materials and methods are available as supplementary materials on Science Online.
15. S. Morein-Zamir, N. A. Fineberg, T. W. Robbins, B. J. Sahakian, *Psychol. Med.* **40**, 263 (2010).
16. J. E. Steinmetz, J. A. Tracy, J. T. Green, *Integr. Physiol. Behav. Sci.* **36**, 220 (2001).
17. G. J. Gage, C. R. Stoetznner, A. B. Wiltchko, J. D. Berke, *Neuron* **67**, 466 (2010).
18. F. Zhang, L. P. Wang, E. S. Boyden, K. Deisseroth, *Nat. Methods* **3**, 785 (2006).
19. N. Mallet, C. Le Moine, S. Charpier, F. Gonon, *J. Neurosci.* **25**, 3857 (2005).
20. P. S. Kalanithi *et al.*, *Proc. Natl. Acad. Sci. U.S.A.* **102**, 13307 (2005).
21. A. H. Gitis, A. C. Kreitzer, *Trends Neurosci.* **35**, 557 (2012).
22. J. R. Crittenden, A. M. Graybiel, *Front. Neuroanat.* **5**, 59 (2011).
23. J. J. Canales, A. M. Graybiel, *Nat. Neurosci.* **3**, 377 (2000).
24. E. Saka, C. Goodrich, P. Harlan, B. K. Madras, A. M. Graybiel, *J. Neurosci.* **24**, 7557 (2004).
25. D. M. Eagle *et al.*, *J. Neurosci.* **31**, 7349 (2011).

Acknowledgments: The authors thank D. Hu, H. F. Hall, C. Keller-McGandy, J. Lee, Y. Kubota, R. MacRae, and D. J. Gibson for their generous help. Funded by the Simons Initiative on Autism and the Brain at MIT (A.M.G. and E.B.); National Institute of Child Health and Development, NIH, R37 HD028341 and Defense Advanced Research Projects Agency, W911NF1010059 (A.M.G.); and National Institute on Mental Health, NIH, R01 MH081201 and Simons Foundation Autism Research Initiative (G.F.). E.B. and A.M.G. designed the experiments, performed data analysis, and wrote the manuscript; E.B. conducted the experiments; P.M. conducted the cell counts; G.F. provided the *Sapap3* mutant mouse model and read the manuscript. The authors declare no competing financial interest. Correspondence and requests for materials should be addressed to A.M.G. (graybiel@mit.edu).

Supplementary Materials

www.sciencemag.org/cgi/content/full/340/6137/1243/DC1
Materials and Methods
Supplementary Text
Figs. S1 to S13
Tables S1 and S2
References (26–32)

5 November 2012; accepted 3 April 2013
10.1126/science.1232380